Nucleic Acids Research, 2025, **53**, gkaf235
https://doi.org/10.1093/nar/gkaf235
Methods

Efficient DNA- and virus-free engineering of cellular transcriptomic states using dCas9 ribonucleoprotein (dRNP) complexes

Tobias Schmidt[1,2], Maximilian Wiesbeck[1,2], Luisa Egert[1,2], Thi-Tram Truong[1,2], Anna Danese[1], Lukas Voshagen[1], Simon Imhof[1], Matilde Iraci Borgia[1], Deeksha[1,2], Andrea M. Neuner[1,2], Anna Köferle[1,2,3], Arie Geerlof[4], André Santos Dias Mourão[4], Stefan H. Stricker[1,2,*]

[1]Reprogramming and Regeneration, Biomedical Center (BMC), Physiological Genomics, Faculty of Medicine, LMU Munich, Grosshaderner Strasse 9, Planegg-Martinsried, 82152, Germany
[2]Epigenetic Engineering, Institute of Stem Cell Research, Helmholtz Zentrum, German Research Center for Environmental Health, Grosshaderner Strasse 9, Planegg-Martinsried, 82152, Germany
[3]Present address: Anna Köferle. Boehringer Ingelheim RCV GmbH & Co KG, Doktor-Boehringer-Gasse 5-11, 1120 Vienna, Austria
[4]Institute of Structural Biology, Helmholtz Centre Munich, German Research Center for Environmental Health, Neuherberg, 85764, Germany
*To whom correspondence should be addressed. Email: stefan.stricker@helmholtz-muenchen.de

Abstract

For genome editing, the use of CRISPR ribonucleoprotein (RNP) complexes is well established and often the superior choice over plasmid-based or viral strategies. RNPs containing dCas9 fusion proteins, which enable the targeted manipulation of transcriptomes and epigenomes, remain significantly less accessible. Here, we describe the production, delivery, and optimization of second generation CRISPRa RNPs (dRNPs). We characterize the transcriptional and cellular consequences of dRNP treatments in a variety of human target cells and show that the uptake is very efficient. The targeted activation of genes demonstrates remarkable potency, even for genes that are strongly silenced, such as developmental master transcription factors. In contrast to DNA-based CRISPRa strategies, gene activation is immediate and characterized by a sharp temporal precision. We also show that dRNPs allow very high-target multiplexing, enabling undiminished gene activation of multiple genes simultaneously. Applying these insights, we find that intensive target multiplexing at single promoters synergistically elevates gene transcription. Finally, we demonstrate in human stem and differentiated cells that the preferable features of dRNPs allow to instruct and convert cell fates efficiently without the need for DNA delivery or viral vectors.

Graphical abstract

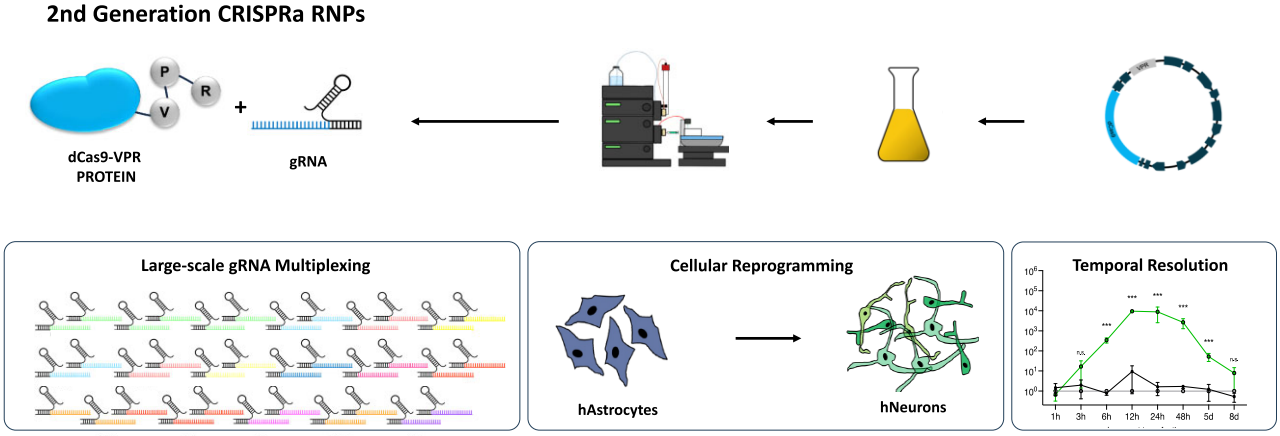

Introduction

Advancements in genome engineering technologies have revolutionized our ability to precisely manipulate genetic material, offering unprecedented opportunities for basic research, biotechnology, and therapeutic applications. Among these technologies, the CRISPR-Cas system has emerged as a

Received: August 14, 2024. **Revised:** March 3, 2025. **Editorial Decision:** March 4, 2025. **Accepted:** March 17, 2025

versatile and powerful tool for targeted genome editing and gene regulation [1–4]. The CRISPR–Cas complex consists of Cas protein responsible for binding the target DNA and a RNA component, defining the target DNA region through complementarity. The RNA component consists either of two small RNAs, the CRISPR RNA (crRNA) and the trans-activating RNA (tracrRNA), or one single guide RNA (sgRNA) [2].

Notably, the simplicity and programmability of CRISPR have facilitated its widespread adoption in various genomic applications [5]. In addition to genome editing, CRISPR has also been harnessed for gene activation using CRISPR activation (CRISPRa) strategies [6–9]. CRISPRa employs a catalytically inactive form of Cas protein (dCas9) fused to one or multiple transcriptional activator domains. In the first generation, single transcriptional effectors (e.g. VP64) were fused to dCas to activate gene transcription [6–8]. In the second generation, the dCas9 is fused to a peptide array that recruits multiple effector copies (dCas9-SunTag-VP64) or RNA aptamers within the gRNA, which recruit a variety of additional transcriptional activator domains (dCas9-SAM) [10, 11]. However, the most commonly used and one of the most efficient second generation CRISPRa systems is dCas9-VPR [12]. Here three trans-activator domains (VP64, p65 and Rta) are directly fused to the C-terminal end of the dCas9-protein, separated by short glycine-serine-linkers. By targeting dCas9–VPR complexes to specific gene promoters or regulatory regions using gRNAs, CRISPRa enables transcriptional activation of endogenous genes without altering their underlying DNA sequences. Therefore, this approach holds immense promise for modulating gene expression profiles in diverse cellular contexts, elucidating gene functions, and engineering cellular phenotypes for biotechnological and therapeutic purposes [5, 13–16].

However, current CRISPRa methods are not always reaching their full potential. First, despite targeted gene activation usually appearing significant and robust, its induction remains often below cDNA overexpression [17, 18]. Consequently, it can remain challenging to recreate cellular gain of function phenotypes, e.g. in cell fate conversion approaches [17, 19, 20], particularly in systems that are not based on immortalized or cancer cell lines. Second, despite the high suitability of CRISPR for gRNA multiplexing in principle, gRNA delivery and/or dCas9 amounts can be limiting, making extensive target multiplexing challenging. Consequently, there are only few examples in which CRISPRa has only been successfully used for a very high number of targets simultaneously (>20) [10, 21, 22]. This makes it currently challenging to use CRISPRa to manipulate transcriptional networks comprehensively. Third, conventional CRISPRa strategies have a low temporal resolution, transcriptional effects appear late and are not reversible when viruses are used or decline non-uniformly in the case of plasmids. Fourth, despite its seemingly straightforward nature, the integration of CRISPRa into diverse delivery systems presents significant challenges. The size of dCas9 fusion proteins often exceed the capacity of viral vectors [23, 24]. Moreover, each novel target site, cell type, or species requires vector cloning and virus generation, while plasmid transfections are notoriously inefficient for many primary cell types.

Wild-type CRISPR RNPs, comprised of Cas proteins and guide RNAs (gRNAs) have been extensively utilized for precise genome editing via induction of targeted DNA double-stranded breaks. The high efficiency and specificity of CRISPR RNPs have made them invaluable tools for functional genomics studies, disease modeling, and therapeutic interventions aimed at correcting genetic mutations underlying various disorders [25–27]. However, efficient protocols for RNP-based secondary CRISPRa systems, particularly for engineering human cells, remain to be established despite their therapeutic potential [13, 14, 28, 29].

Here we develop an RNP-based CRISPRa approach using the potent transcriptional activator VPR. We demonstrate that highly active dCas9-VPR protein can be efficiently purified from insect cells with high yields and that it is able to assemble with cRNAs to form functional dCas9-VPR-ribonucleoprotein-complexes (dRNPs). Delivery of dRNPs into human stem cells, differentiated progeny and primary cells is highly efficient. We show that targeted gene induction is extremely effective (up to 10^5-fold) even for silenced developmental transcription factor genes. Characterization of the effects reveal that the dRNP-based gene induction is rapid and transient. After defining an optimal dose, we show that dRNPs enable the effective simultaneous activation of at least 11 transcription factor genes by applying 22 gRNAs, without loss of efficacy. We further show that increasing the number of gRNAs targeting gene regulatory elements of one gene boosts transcriptional output synergistically. Finally, we demonstrate that the effectiveness of dRNPs makes it applicable to induce cell fate instruction and cell fate conversion in human stem and differentiated cells.

Material and methods

dCas9-VPR protein production and purification

For protein expression in insect cells, the dCas9-VPR sequence was first cloned into the donor vector (pFastBacHT). dCas9-VPR protein was produced in *Spodoptera frugiperda* Sf21 cells. First, recombinant viral DNA was generated to infect the insect cells. The donor plasmid containing the dCas9-VPR (pFastBacHT_A-1_dCas9VPR) was transformed into *Escherichia coli* DH10Bac cells containing a transposase and the viral DNA (bacmid). Through blue-white screening, a colony was selected. The bacmid was isolated and transfected to Sf21 cells to produce recombinant virus. Around 1.0×10^6 cells were infected with the virus, ans they were harvested after 3 days, pelleted and frozen at −20°C until further use.

The cell pellet was resuspended in lysis buffer (20 mM Tris pH 8.0, 200 mM NaCl, 5% glycerol, 10 mM imidazole) and applied on a Ni-NTA raisin column to isolate the *N*-terminal 6xHis-tagged protein by gravity flow. The column was washed twice with lysis buffer, once with 1M NaCl, and again with lysis buffer. Proteins were eluted with high concentrations of imidazole (lysis buffer + 350 mM imidazole).

The salt concentration was adjusted to 100 mM NaCl before the eluate was injected to the HiTrap Q HP column (Cytiva) using the ÄKTApurifier system (GE Healthcare). The column was equilibrated to Buffer A (20 mM Tris pH 8.5, 100 mM NaCl, 1 mM $MgCl_2$), and the protein was eluted with a 50% gradient of Buffer B (20 mM Tris pH 8.5, 1000 mM NaCl, 1 mM $MgCl_2$). Fractions were collected and concentrated.

As a final purification step, the protein was injected onto the Superose 6 (Cytiva) size-exclusion column operated by the ÄKTApurifier system (GE Healthcare). The protein was eluted with a flow rate of 0.5 mL/min of SEC buffer (20 mM Tris pH 7.5, 200 mM NaCl, 5% glycerol, 1 mM β-mercaptoethanol).

Protein fractions were identified by SDS-PAGE, pooled, flash frozen, and stored at -80°C. Protein concentration was determined by the absorption at 280 nm.

dCas9-VP64, purified from *E. coli*, was a gift from Prof. Rasmus O. Bak (Aarhus University). As for dCas9-VPR, the dCas9-VP64 is derived from the *Streptococcus pyogenes* sequence [29]. Those protein differ by dCas9-VPR containing a 6xHis- and a FLAG-tag, a TEV site, two SV40 nuclear localization signals, and three short linker sequences, while dCas9-VP64 contains one Nucleoplasmin and one SV40 nuclear localization signal, as well as two longer linker sequences [29].

Human stem cell culture

The human stem cell culture (hiPSC) line used in this study (HMGU-1) has been generated by the iPSC core unit of the Helmholtz Zentrum München. The cells were cultured in mTeSR1 containing 1x mTESR1 supplement (Stem Cell Technologies) on six-well-plates coated with Geltrex™ (Gibco). iPSCs were cultured for ∼30–35 passages. When the cells reached ∼80–90% confluency, they were split to Geltrex™-coated cell culture dishes.

Generation of human proliferating astrocytes

Human proliferating astrocytes (pAstros) were generated as previously described [30]. In brief, human iPSC were dissociated with collagenase and cultured as embryoid bodies (EBs) in mTeSR1 containing 1x mTESR1 supplement (Stem Cell Technologies) supplemented with Rock Inhibitor Y-27632 (10 μM) (Stem Cell Technologies). The following day, media was changed and EBs were cultured in Astrocyte medium (AM) supplemented with 20 ng/ml Noggin (Peprotech) and 10 ng/mL PDGFAA (R&D Systems) for 2 weeks. After an additional week in AM supplemented with only 10 ng/mL PDGFAA, EBs were mechanically dissociated and plated to POL-coated dishes. Resulting pAstros were cultured in AM supplemented with bFGF (10 ng/μl) (Peprotech) and EGF (10 ng/μl) (Peprotech) for ∼40 days. Cells were passaged using Accutase (Thermo Fisher Scientific), and media was continuously replaced every second day.

Human adult dermal fibroblasts

Human adult dermal fibroblasts (HAFs, Lonza CC-2511) were cultured in Advanced DMEM (ADMEM) supplemented with 5% FBS and penicillin/streptomycin (P/S) or in fibroblast growth basal medium (FBM) (Lonza) on gelatine (ROTI-Cell)-coated plastic cell culture dishes or on PDL (poly-D-lysine (Sigma)) or PDLL (PDL and laminin (Roche))-coated glass-coverslips at 37°C, 5% CO_2. When reaching ∼80% confluency, cells were passaged by washing once with 1 x phosphate-buffered saline (PBS) followed by incubation with 0.05% Trypsin (Gibco) for 5 min at 37°C. Cells were counted either manually using a microscope or by using the Countess™ Cell Counter (Thermo Fisher Scientific).

gRNA design

For endogenous gene activation via dRNPs, targeting sites were considered within 1-kb upstream of the transcriptional start site (TSS) of the target gene and prioritized by proximity to the TSS. The gRNA design tool, CHOPCHOP, was used using standard settings for gene activation [31] or gRNAs were picked manually from CRISPR tracks via the UCSC genome browser. When multiple gRNAs were used, a distance of at least 80 bp was kept between gRNAs, if possible. Single gRNAs (sgRNA), crRNAs, tracrRNAs, and crRNAs stabilized through undisclosed chemical modifications (crRNA_XT) have been obtained from commercial sources (IDT).

HEK293T cells

HEK293T cells were cultured in DMEM medium supplemented with 5% FBS and penicillin/streptomycin (P/S). When reaching ∼80% confluency, cells were passaged by washing once with 1 x PBS followed by incubation with 0.05% Trypsin (Gibco) for 5 min at 37°C. Media was changed every second day.

Nucleofection

For nucleofections, 10^6 hiPSCs were used per condition according to the manufacturer's instructions (Lonza™ P3 Primary Cell 4D-Nucleofector™ X Kit L). Cells were collected and resuspended in 82 μl P3 Primary Cell Nucleofector Solution and 18 μl Supplement 1. DNA was added and the mix was transferred to Nucleocuvettes. Nucleofection was performed using the program CA 137. Around 500 μl of RPMI medium was added and ells were incubated for 15 min at 37°C, 5% CO_2 for recovery. Around 120 μl cell suspension was added per well to a Geltrex-coated 24-well plate (Thermo Fisher Scientific A1413302) containing 500 μl pre-warmed mTeSR™1 media (Stemcell 85 850). Cells were maintained at 37°C, 5% CO_2 until analysis.

dCas9-VPR RNP (dRNP) assembly and delivery

First, crRNA:tracrRNA duplexes were formed by mixing crRNA with tracrRNA (Alt-R® CRISPR-Cas9 tracrRNA, ATTO™, IDT) in equimolar ratio, diluted in Nuclease-free Duplex Buffer (IDT) to 2 μM and incubated at 95°C for 5 min. After 10 min cooldown, per 1.000.000 cells, 50 μl of crRNA:tracrRNA duplex (2 μM) was mixed with 50 μl dCas9-VPR protein (2 μM), diluted in Opti-MEM to 0.12 μM, and incubated for 10 min for RNP assembly. When multiple gRNAs were used per condition, RNPs were mixed prior to delivery. Assembled dRNPs were directly transfected using RNAiMAX Transfection Reagent (Thermo Scientific) (20 μl per 10^6 cells) or delivered via nucleofection using the 4D Nucleofector® (Lonza). Following dRNP delivery, cells were incubated at 37°C, 5% CO_2 and media was changed after 16–20 h.

dRNP multiplexing

For multiplexing experiments, dRNPs were prepared separately for individual gRNAs until delivery. To determine dRNP multiplexing limits (Fig. 4 and Supplementary Fig. S5), 5 pmol per gene and 10^5 cells were used, independently of the experimental condition. Total amounts transfected were 5 pmol (single), 25 pmol (Set1), 30 pmol (Set2), 55 pmol (22_gRNAs), or 75 pmol (35 gRNAs). For the experiments on gRNA synergism (Fig. 5) and the direct neuronal conversion (Fig. 7), the total amount of dRNPs transfected was 10 pmol per 10^5 cells in each condition.

Human iPSC to neuron differentiation

One day prior to transfection and transduction, human iPSCs were seeded at a density of 80′000 cells per well on a 24-well plate coated with Geltrex™ (Gibco). The next day, cells were transfected with dRNPs (10 pmol per 10^5 cells). One day after transfection, media was changed to mTeSR1 containing 1x mTESR1 supplement (Stem Cell Technologies). On day 4 of the experiment, media was changed to N3 medium containing DMEM/F12 and Neurobasal media (1:1) supplemented with P/S (1x), B27 supplement (1x), N2 supplement (1x), MEM non-essential amino acids (NEAA) (1x), GlutaMAX (1x), ß-mercaptoethanol (50 μM), Insulin (2.5 μg/mL), Dorsomorphin (1 μM), and SB431542 (10 μM). Media was changed daily. On day 6, cells were fixed with 4% paraformaldehyde (PFA) for 15 min and analyzed via Immunostaining. The cultures were maintained at 37°C, 5% CO_2, and 5% O_2.

Human pAstros to neuron reprogramming

Human pAstros were plated at a density of 40 000 cells per well on POL-coated 24-well plate. The next day (d0) and 3 days after (d3), cells were transfected with dRNPs targeting the promoter region of *NEUROG2*, *NEUROD1* or multiplexed activation of *NEUROG2*, *NEUROD1*, and *NEUROD4* (NNN). A total of 10 pmol per 10^5 cells for all conditions was used. Two days after the first transfection (d2), to support neuronal conversion, full media was changed neuronal reprogramming media (NRM) consisting of DMEM/F12 and Neurobasal media (1:1) supplemented with P/S (1x), B27 supplement (1x), N2 supplement (1x), and MEM non-essential amino acids (NEAA) (1x). The following small molecules were added:(30) LM-22A4 (2 mM), LDN-193189 (0.5 mM), CHIR99021 (2 mM), SB-431542 (10 mM), Noggin (50 ng/ml), GDNF (2 ng/ml), NT3 (10 ng/ml), and db-cAMP (0.1 mg/ml). Half of the media was changed every second day. From days 17 to 20 of the experiment, the NRM was only supplemented with LM-22A4 (2 mM), GDNF (2 ng/ml), NT3 (10 ng/ml), and db-cAMP (0.1 mg/ml). On day 20, cells were fixed with 4% paraformaldehyde (PFA) for 15 min and analyzed via Immunostaining. The cultures were maintained at 37°C, 5% CO_2, and 5% O_2.

Retrovirus transduction

As a positive control for human iPSC to neuron differentiation, cells were transduced with 1 μl (10^8–10^9 particles/ml) of virus per well. The viral construct contains a phosphoincompetent form of *NEUROG2* (Ngn2) under control of the CAG promoter as used before [30]. After 1 day, transduction media was changed, and cells were treated in parallel to the dRNP conditions, as described above.

Flow analysis and fluorescence-activated cell sorting

For flow analysis or cell sorting, cells were washed once with 1 x PBS and detached by using detachment reagents appropriate for the cell type. After incubation for 5 min at 37°C, the reaction was stopped by adding double the amount of cell culture media, and cells were collected in 15 ml tubes. The cells were centrifuged for 5 min at 300 x g and supernatant was removed. Cell pellets were resuspended in 1 ml 1x PBS and filtered (40 μm) into fluorescence-activated cell sorting (FACS) tubes. For cell sorting, a FACSAriaIII™ (Becton Dickinson) device at a flow rate of 1 (arbitrary units) was used according to the manual. The fluorescence intensity of the ATTO550-labeled tracrRNA was used for gating, the mock transfected or control cells served as reference. For each target, 10^5 cells were sorted into a 1.5 mL tube for RNA isolation and RT-qPCR analysis.

RNA isolation and cDNA synthesis

RNA isolation was performed by using the Total RNA Miniprep Kit (Monarch™) according to the manufacturer's protocol. In short, 300 μL Lysis Buffer (NEB) was added to the cell pellet containing 10^5 cells. Around 300 μL of 100% ethanol was added to the lysate and mixed thoroughly, and RNA was isolated following the manufacturer's protocol. The RNA concentrations were measured on a spectrophotometer (NanoDrop) using H_2O as a reference. Around 100 ng RNA were used for cDNA synthesis using the Maxima first strand cDNA synthesis kit (Thermo Scientific).

Real-time quantitative PCR (RT-qPCR)

Gene expression levels were analyzed through Real-Time quantitative PCR (RT-qPCR) on an QuantStudio™ 6 Flex Real-Time PCR (Applied Biosystems) System using PowerUp™ SYBR Green Master Mix (Thermo Fisher Scientific). cDNA from 100 ng RNA were diluted 1:5 in H_2O. For each target gene, a master-mix containing 5 μL PowerUp™ SYBR Green Master Mix and 0.05 μL of both forward and reverse qPCR primers (10 μM) per reaction was prepared. Each condition was analyzed as technical triplicates. Additionally, one control reaction (-RT) and a H_2O control for each master-mix were included to check for false positive amplification of remaining genomic DNA. For quantitative comparison of expression levels, each sample was analyzed relative to technical triplicates of expression levels of the house keeping gene GAPDH. 5 μL of the gene-specific master-mix was dispensed into a 384-well plate, followed by addition of 5 μL of the respective cDNA. Amplification was performed with an QuantStudio™ 6 Flex Real-Time PCR System. The resulting Ct-values were exported, and quantitative gene expression levels were determined as described [32].

Immunocytochemistry

For immunocytochemical analysis, cells were cultured on PDL or POL-coated glass coverslips in 24-well plates. The cells were fixed with 4% paraformaldehyde (Sigma) for 15 min at room temperature and washed three times with PBS. Unspecific binding sites were blocked with blocking solution (BS) (3% BSA (Sigma) and 0.5% Triton X-100 (Merck) in PBS) for 1 h at room temperature. Primary antibodies were diluted in blocking solution and added to the fixed cells for overnight incubation at 4°C. The coverslips were washed three times with 1 x PBS and incubated with secondary antibodies as fluorophore conjugates, diluted in BS together with DAPI (Tocris, 1:1000) and incubated for 2 h at room temperature. After three times washing with 1 x PBS, the coverslips were mounted onto microscope glass slides using Aqua-Poly/Mount (Polysciences).

Microscopy and image acquisition

Immunofluorescence stainings were analyzed using a LSM 710 laser scanning confocal microscope (Zeiss). Laser inten-

sities were adjusted to the control coverslips as reference. Images were taken with a 40X water immersion objective. A bit depth of 12 was chosen and averaging was performed in line mode (bi-directional) as the mean from two acquisitions. Tile scans with 10% overlap were taken for cell counting and stitching (strict, 0.90) was performed. Images were exported as czi-files and further processed with Fiji [33].

Western blotting

At least 10^5 cells per experimental condition were lysed using RIPA buffer (Sigma-Aldrich R0278). Protein concentration was determined via the Lowry method using Dc Protein assay kit (Biorad 5 000 111). Around 30 µg of protein was loaded on a 10% sodium dodecylsulphate-polyacrylamide gel electrophoresis gel using Acrylamide/Bis solution (37.5:1, Biorad 161–0148), 10% APS (Sigma A3678-25G), TEMED (Sigma T-9281), Precision Plus protein All Blue Standards (Biorad 161–0373). Following gel electrophoresis blotting was performed on a methanol-activated 0.2-µm polyvinylidene membrane (ThermoFisher LC2002). Membranes were blocked in 5% milk in 1 × TBST (Tris-buffered saline with Tween20) and incubated overnight with primary antibody (see Supplementary Table). The next day, membranes were washed in 1 × TBST three times and incubated with HRP (Horseradish Peroxidase) conjugated antibodies for 2 h. Membranes were washed in 1 × TBST three times. For detection, the ECL system was used (Luminol Reagent, Santa Cruz Biotechnology sc-2048).

Bulk RNA sequencing

Before mRNA sequencing, integrity of RNA samples was estimated (RIN > 7). Libraries were prepared using the Illumina Stranded mRNA Prep Ligation kit with an input of 1000 ng following to the kit instructions. After QC, the libraries were sequenced in paired-end mode (2 × 100 bases) on the NovaseqX + sequencer (Illumina) at a depth of ≥30 million reads per sample. The initial data processing started by trimming sequencing primers using trimmomatic v0.39 [34]. Then the fastqs are aligned with STAR v2.7.10b [35], using GRCh38 v47 from Gencode as reference genome. PCR duplicates are removed using samtools rmdup v1.6 [36]. Finally the count matrices are built using htseq v0.11.3 [37]. Transcripts present in <3 samples were filtered out. Sequencing coverage was normalized using TPM. The analysis was performed using python v3.9.15 and the following packages decoupler 1.8.0 [38], scanpy 1.10.1 [39], anndata 0.10.7 [39], and pydeseq2 0.4.12 [40]. The RNA-Seq data have been deposited in GEO under the accession number GSE288075. Raw data are available upon request.

Data analysis and quantification

Data were quantified using Microsoft Excel. Graphs were created with GraphPad Prism 9.0, and statistical analysis was carried out in GraphPad Prism 9.0 and RStudio. For statistical analysis of gene induction levels, log-fold change values were calculated from RT-PCR data. The efficiency of dRNP mediated pAstros to neuron conversion was quantified from immunocytochemistry (ICC) images at d20 of the experiments. For each independent experiment, different treatments were analyzed from 2 to 3 coverslips. 2 × 2 or 3 × 3 tile scans at 40X magnification were taken resulting in ∼500–1000 dapi positive cells which were analyzed per coverslip. Supplementary methods are found online (Supplementary Information).

Results

Generation of dCas9-VPR ribonucleoprotein-complexes

The objective of this study is to develop strategies and protocols for the generation and use of CRISPR RNPs, aiming to enhance the efficiency of CRISPRa strategies for targeted gene induction. These improvements are a prerequisite to facilitate cell fate instruction and reprogramming with CRISPRa in human primary and stem cells effectively. Thus, the challenge includes to produce significant amounts of full-length protein of a powerful second generation CRISPRa protein, as well as to develop conditions for its efficient delivery and use. Since we and others failed to purify dCas9-VPR protein from bacterial cultures [29], we employed a system based on *Spodoptera frugiperda Sf21* insect cells (Methods, Supplementary Methods S1, and Fig. 1A). With this approach, we achieved strong expression of full-length protein and yielded significant amounts of pure 6xHis-dCas9-VPR protein by Ni-NTA affinity chromatography followed by anion exchange and size-exclusion chromatography purification steps (Supplementary Fig. S1).

dCas9-RNPs can be delivered to various cell types with high efficiencies

Next, we quantified the compatibility of dRNPs with various human cell types using lipofection (Supplementary Fig. S2 and Methods). For this, we made use of a fluorescently labeled tracrRNA (ATTO550, IDT) and ICC making use of a FLAG-tag on the protein to estimate the efficiency of delivery of the dRNPs. First, 20 pmol (per 10^5 cells) of dCas9-VPR protein was assembled with crRNA:tracrRNA duplex RNAs and transfected into human adult fibroblasts (HAF) (see Methods, Fig. 1A). One day after delivery, we observed fluorescence signals in the nucleus of the vast majority of cells (>90%), indicative of CRISPR RNPs entering cells and nucleoplasm efficiently. Furthermore, we did not notice elevation of cellular stress or death (Fig. 1B). Even three days after delivery a vast majority of HAF cells (∼98%) appeared fluorescently labeled using flow cytometry, indicating a very high delivery rate (Fig. 1C).

RNP-based CRISPRa leads to strong and rapid induction of target genes

To investigate the potential of the RNP-based approach for gene regulation, we designed gRNAs and applied published sequences to target the promoter regions of a set of neuronal transcription factors, with active roles in cell identity determination (Fig. 2A and B, Supplementary Fig. S3A, Supplementary Methods S2) [5, 41]. For each target gene, two gRNAs were combined, to increase coverage of the transactivating proteins on the promoter region (Supplementary Fig. S3A) [12]. Three days after dRNP transfection (20 pmol/10^5 cells), mRNA levels were determined via RT-qPCR. We observed strong upregulation of all tested target genes. Indeed, induction of *NEUROD1*, *ASCL1* and *NEUROG2* exceeded several log scales in HAFs (Fig. 2A), but also other human cell types, such as pAstros cultures (Fig. 2B) and human induced pluripotent stem cells (iPSCs (Fig. 6D). The detected in-

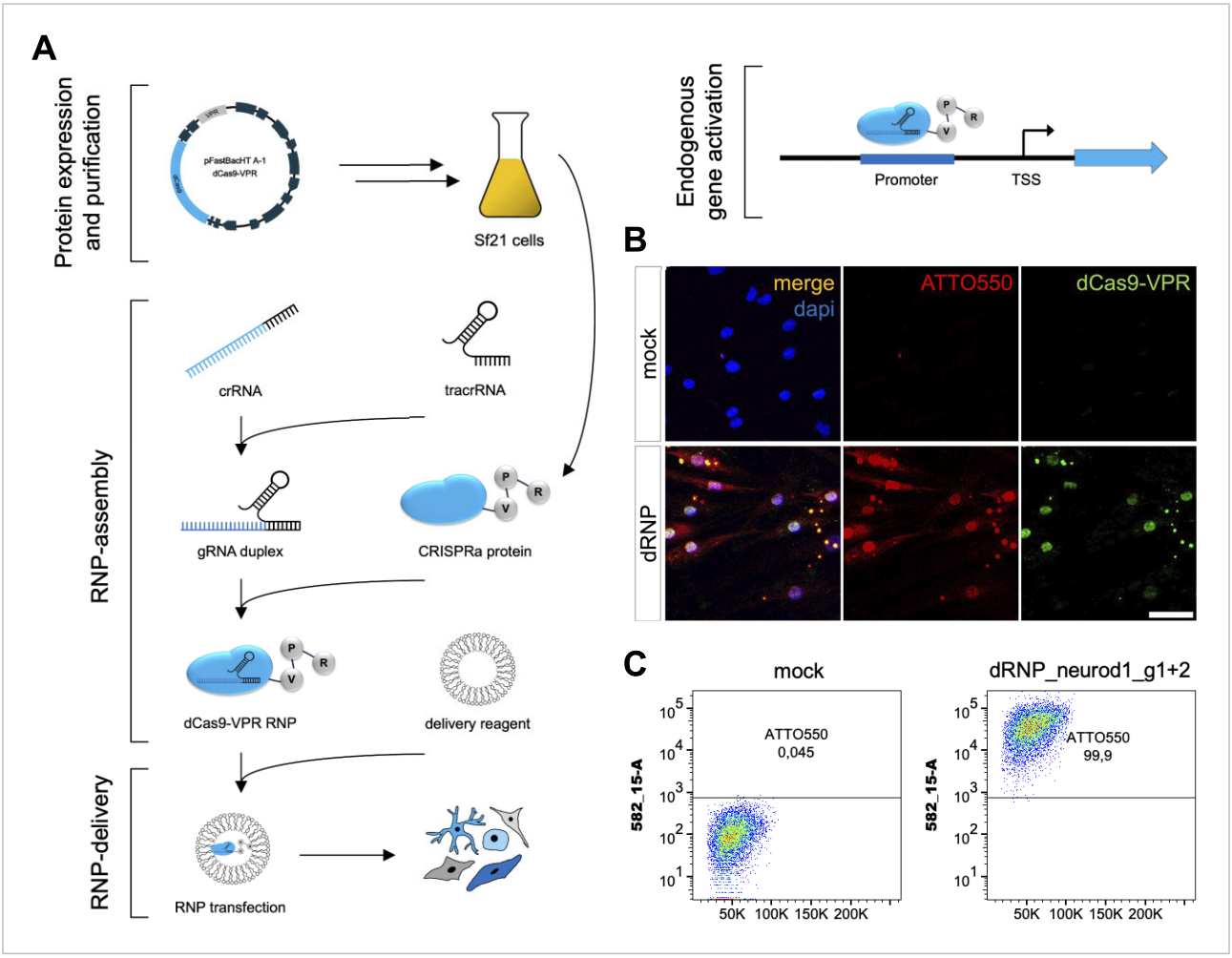

Figure 1. dCas9-VPR is purified from insect cells in high yields and allows to form CRISPRa–RNP complexes (dRNPs), which are delivered to human cells with high efficiencies. (**A**) Method overview. (**B**) Immunifluorescence microscopy images showing the destination of the dRNPs 24h after transfection of HAFs. dRNPs are visualized through the fluorophore ATTO550 labeled tracrRNA and stained for the FLAG-tag as part of the dCas9-VPR protein. Scale bar: 50. (**C**) Flow cytometry analysis of the RNP uptake 3-day post-delivery. Transfected HAF cells were analyzed and sorted through the ATTO550 labeled tracrRNA as part of the dRNP complex. Mock transfections were used as negative controls.

duction exceeded the transactivating effect of first generation CRISPRa RNPs, purified from *E.Coli* (gift from Prof. Rasmus O. Bak, Fig. 2C), as well as established CRISPRa plasmids, containing expression cassettes for dCas9-VPR and target sequence-identical gRNAs, delivered side-by-side by lipofection (Fig. 2D) [29, 42]. A part of the enhancement of transactivation compared to plasmid based system is likely due to the efficiency of dRNP delivery, since nucleofection narrowed the gap (Fig. 2D). To test the robustness of RNP-mediated gene activation strategies, we compared gene induction of complexes targeting two neural fate factors, *NEUROD1* and *NEUROG2*, with several independent batches of dCas9-VPR protein purification and gRNAs. Reassuringly, induction rates were comparable indicating a high robustness of the method (Supplementary Fig. S3B and C).

To estimate off-target effects of dRNP approaches, we next conducted RNA-seq analysis. To reduce the number of secondarily regulated genes we switched the target from TFs such as *NEUROD1* or *NEUROG2* to the cell-adhesion molecule EPCAM. Reassuringly, the transcriptome analysis showed that only a handful of genes are substantially changed, while *EPCAM* shows indeed the highest transcriptional upregulation (Fig. 2E). Among the other elevated genes are several with roles in extracellular matrix, cell contacts and adhesion (such as Matrix metalloproteinase-25, Collagen Typ IX, alpha 3 and the actin binding protein LBD3), indicating their elevation is likely a consequence of *EPCAM* induction, which can regulate gene activity in various ways [43]. In line with this, none of these genes had predicted binding sites for used gRNAs (four mismatches or less) using CRISPOR [44], and none of the Top10 predicted off-target genes showed significant elevation (over two-fold) in the RNA-seq.

To characterize the temporal resolution of the RNP-based CRISPRa system, we transfected active dRNP complexes targeting two neuronal TFs (*NEUROD1* and *NEUROG2*) into HAF cells and determined mRNA levels between one hour and eight days post-delivery (Fig. 3A). Interestingly, already 3–6 h after dRNP delivery significant elevation of target mRNA levels is apparent, the maximal induction is reached shortly thereafter (~12–24 h, Fig. 3A). Moreover, mRNA levels started to decline between 24 and 48 h (Fig. 3A). In line with these findings, a rapid decrease of dCas9 protein after transfection was detected via western blot (Supplementary Fig. S3D). This indicates that dRNPs allow to engineer transcriptional induction

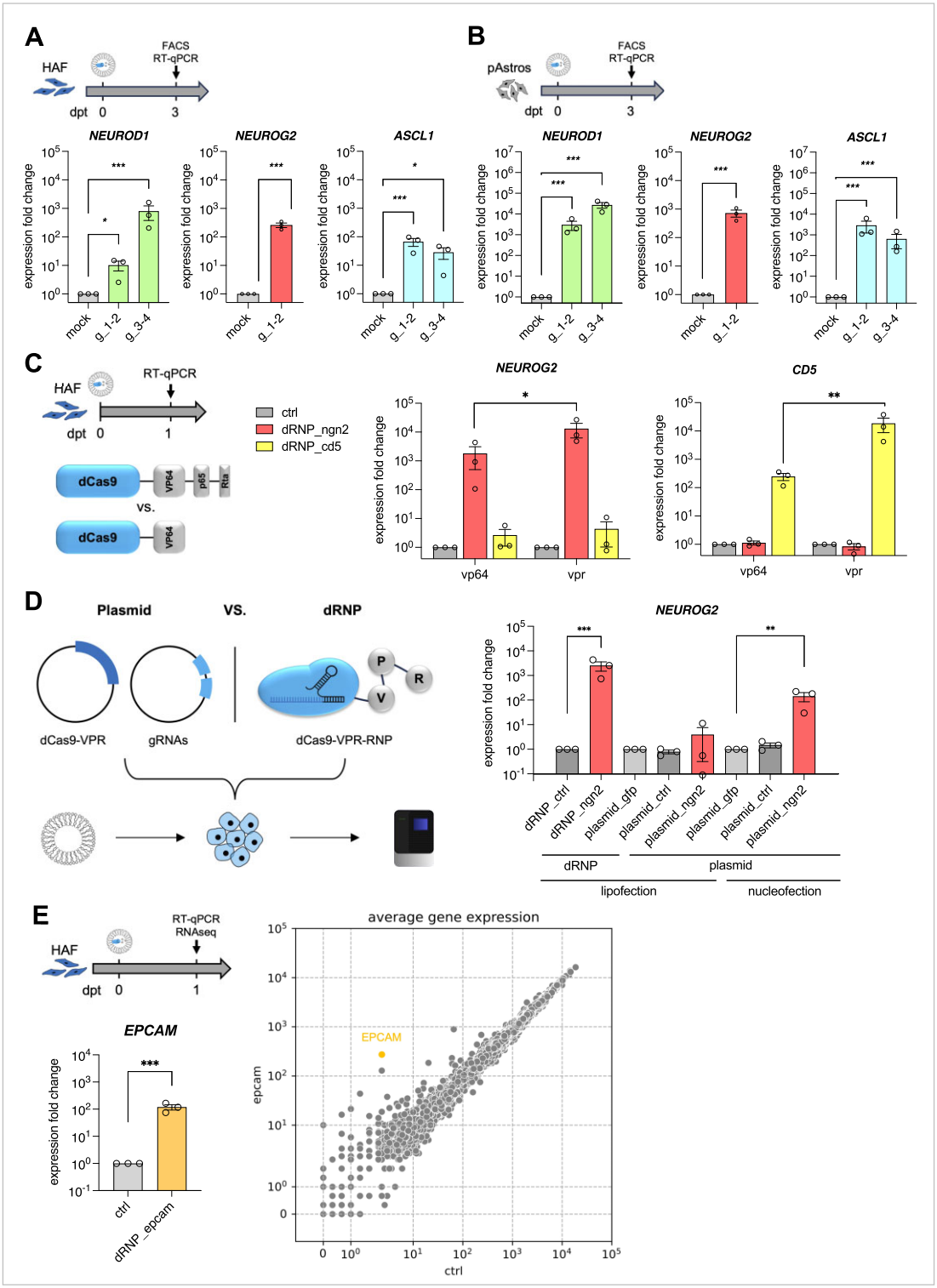

Figure 2. dRNPs strongly induce target genes in human primary cells. **(A** and **B)** dCas9-VPR-RNP induced gene expression of human reprogramming factor genes measured by RT-qPCR 3 days after transfection in HAF (**A**) and human iPSC-derived proliferating astrocytes (pAstros) (**B**). For each target, combinations of two gRNAs targeting the promoter regions of the genes were used. Data are presented as mean ± S.E.M. ($n = 3$ independent experiments). Two-tailed t-test was performed for statistical analysis. * $P < 0.05$, ** $P < 0.01$, *** $P < 0.001$. (**C**) Side-by-side comparison of dRNP-based CRISPRa using dCas9-VPR or dCas9-VP64 [29]. RNPs were prepared equally, using either two (*NEUROG2*) or three (*CD5*) gRNAs to target the endogenous promoter of the genes. RT-qPCR analysis was performed 1 day after delivery. Data are presented as mean ± S.E.M. ($n = 3$ independent experiments). Two-tailed t-test was performed for statistical analysis. * $P < 0.05$, ** $P < 0.01$. (**D**) Comparison of dRNPs with DNA-based CRISPRa. DNA vectors expressing dCas9-VPR or two gRNAs targeting *NEUROG2* were co-delivered by transfection or nucleofection and compared to dRNP-based delivery via transfection. Data are presented as mean ± S.E.M. ($n = 3$ independent experiments). Two-tailed t-test was performed for statistical analysis. ** $P < 0.01$, *** $P < 0.001$. (**E**) RT-qPCR and full transcriptome analysis (RNAseq) one day after dRNP delivery to HAF cells targeting upregulation of the non-TF gene epithelial cell adhesion molecule (*EPCAM*) using two gRNAs. Data are presented as mean ± S.E.M. ($n = 3$ independent experiments). Two-tailed t-test was performed for statistical analysis. *** $P < 0.001$.

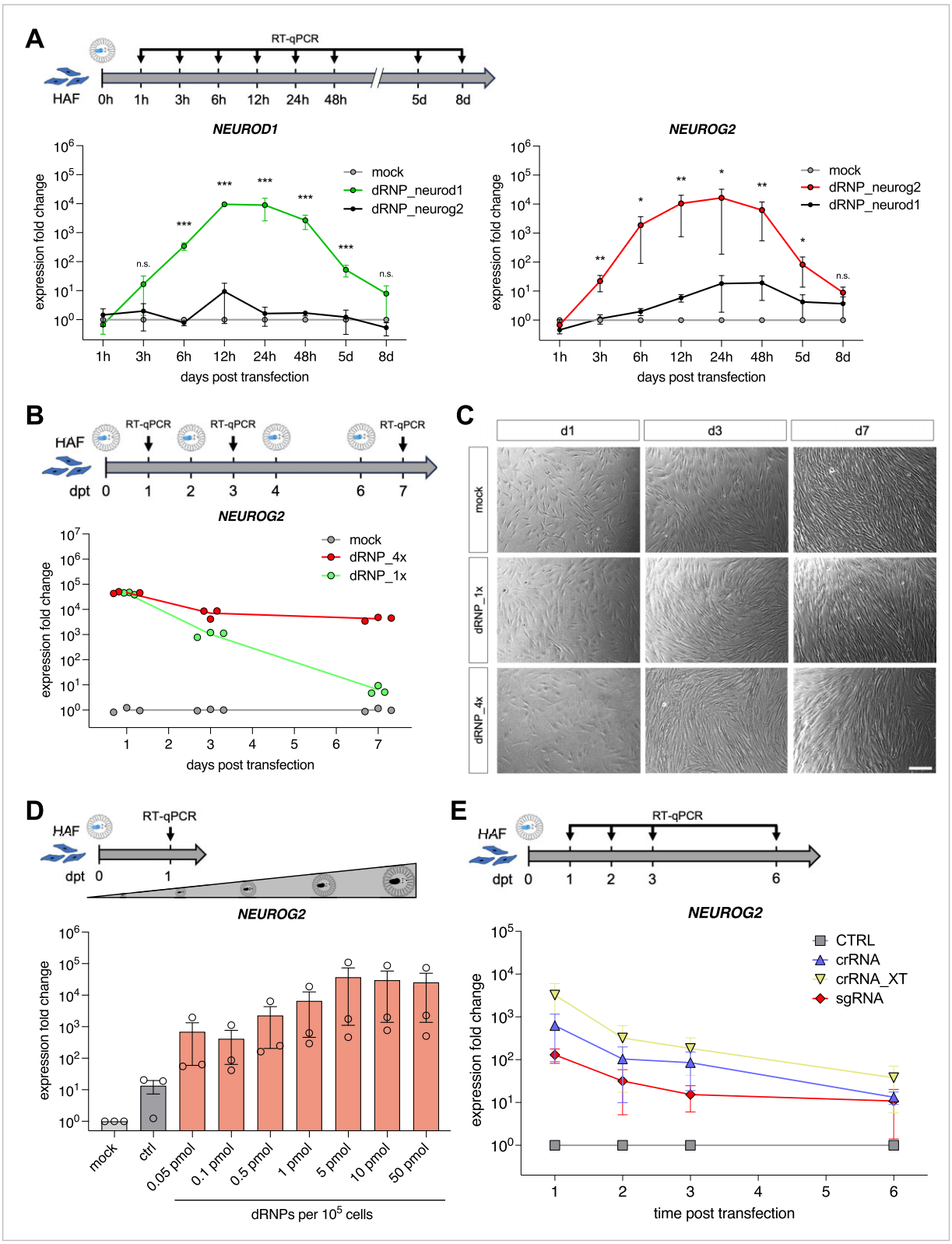

Figure 3. Characterization of dCas9-VPR-RNP-based gene regulation in HAFs. (**A**) Experimental design and RT-qPCR time-course analysis of dRNP-based gene regulation. dRNPs were delivered once to target either NEUROD1 or NEUROG2 and RNA was collected between 1 h and 8 days post transfection, followed by RT-qPCR for analysis. Data are presented as mean ± S.E.M. ($n = 3$ independent experiments). Two-tailed t-test was performed for statistical analysis. * $P < 0.05$, ** $P < 0.01$. (B,C) Effects of consecutive dRNP delivery on gene transcription and cell viability. dRNPs were either delivered once (dRNP_1x) or four times within 6 days (dRNP_4x) and target gene levels (*NEUROG2*) were determined via RT-qPCR (**B**). Representative brightfield images throughout the experiment allowed to demonstrate cell survival (**C**). Data points represent independent ($n = 3$) experiments. Scale bar: 200 μm. (**D**) Dose-dependent effect of RNP-based transcriptional activation (amounts indicated as pmol dRNPs per 10^5 cells at delivery). Data are presented as mean ± S.E.M. ($n = 3$ independent experiments). (**E**) Comparison of different types of RNAs to evaluate the effect on RNP stability and target gene expression. Data are presented as mean ± S.E.M. ($n = 3$ independent experiments).

more effective and with temporal resolution on par with comparable systems for endogenous gene induction applying optogenetics [45–47]. To test, whether dRNP treatment can be repeated to prolong transcriptional induction, if intended, we transfected human fibroblast cultures once or four times with dRNPs targeting the transcription factor NEUROG2 over the period of 7 days (Fig. 3B). While both conditions highly induced the target gene after 24 h, only repeated delivery resulted in elevated expression after 1 week, without apparent increase of cellular stress or cell death (Fig. 3C).

Determining optimal complex conditions for RNP-mediated CRISPRa

To determine the efficacy of our dRNPs further and to avoid potential protein overload eliciting adverse responses such as unfolded protein response (UPR) [30], we determined the minimal effective dose of RNPs. For this, we delivered different amounts of RNPs (50 fmol – 50 pmol) into 10^5 HAF cells. Interestingly, even the lowest tested dose activated *NEUROG2* expression in these cells over 2–3 log scales (Fig. 3D). Increasing the amount of RNPs further revealed an approximately linear dose response relation, until the expression plateaus using 5 pmol per 10^5 cells or higher, resulting in 10^4–10^5-fold gene induction (Fig. 3D). This result was also in line with the finding that reducing gRNA amount substoichiometrically to a third did not reduce transcriptional induction (Supplementary Fig. S3E). However, flow cytometry analysis applying fluorescently labeled tracrRNA indicated further, that RNP amounts lower than 5 pmol lowered RNP delivery rates (Supplementary Fig. S4A). To test whether the upper limit of RNP mediated activation effects is gene dependent, we repeated the experiments with medium to high concentrations (10–80 pmol for 10^5 cells) of RNP complexes targeting three different neural fate transcription factor genes (*NEUROD1*, *NEUROG2* and *ASCL1*) and found that higher doses did not further increase transcriptional output of either gene (Supplementary Fig. S4B) but had a tendency to impair cell viability (Supplementary Fig. S4C).

Next, we tested whether gRNA structure and stability have major impact on the transcriptional induction mediated by CRISPRa RNPs. For this, we compared three different available gRNA types each targeting the same two sequences within the human *NEUROG2* promoter (Supplementary Fig. S3A). We tested sgRNA, crRNAs stabilized through chemical modifications (crRNA_XT, IDT) and standard crRNA:tracrRNA duplex gRNAs (crRNA). While crRNA_XT induced *NEUROG2* immediately (d1) higher (∼5-fold) compared to the duplex gRNAs, which was used before, the commonly used sgRNAs performed substantially worse (Fig. 3E) indicating that RNP-mediated gene induction can be profoundly affected by the gRNA type used. The transcriptional induction retained a high temporal resolution in all cases and more effective complexes, such as those build with crRNAs_XT, did not result in a decelerated relative decline of *NEUROG2* mRNA over 3–6 days. This indicates that the temporal dynamics after 24 h is likely mostly defined by the half-life of *NEUROG2* mRNA produced during the first 24 h (Fig. 3E).

Determining multiplexing limits for RNP mediated CRISPRa

To investigate the potential of RNPs to induce multiple target genes, we designed 22 crRNA:tracrRNA duplex gRNAs targeting 11 neural transcription factor genes (Fig. 4A). Next, we delivered specific RNP complexes either on their own, or in combination in sets of five, six, or all eleven target genes. Interestingly, we found that the application of 22 duplex gRNAs into HAF cells did overall not reduce the activation potential of each individual one (Fig. 4B). This was the case for genes with high (*NEUROD1*, *NEUROG2*, *ASCL1*, *NEUROD4*, *BRN2*), medium (*SOX1*, *FOXG1*), and low (*SOX4*, *CUX1*) transcriptional activation rates, indicating that dRNP mediated target gene induction supports multiplexing at levels comparable to the highest numbers reported to date, e.g. using dCas12 crRNA, dCas9 gRNA expression vectors, or viral delivery systems [5, 22, 48, 49]. Interestingly, one gene (*PAX6*), which only showed limited response to CRISPRa, reached however higher mRNA levels the more other neural TFs have been induced, suggesting a potential indirect effect (Fig. 4B). Moreover, even excessive multiplexing combining 35 gRNAs resulted in high induction of individual target genes, although in this setting, combined inductions did not fully reach the levels of individual gene targeting (Supplementary Fig. S5).

For targeted gene activation, most commonly few gRNAs per gene have been used [7, 8, 10, 50]. This has several reasons; some are biological in nature, since with increasing distance from the TSS gRNAs have not only been shown to be less effective [9, 10] but also methodological, since higher numbers of gRNA expression constructs are more difficult to generate and delivery is less effective using plasmid and virus based systems. Since with the dRNP-based system, comprehensive gRNA multiplexing seemed to be straightforward, we next investigated, whether increasing number of gRNAs targeting one single gene promoter would significantly affect gene expression. To test this hypothesis, we designed eight different gRNAs targeting the *NEUROD1* core promoter, between 50- and 500-bp upstream (gRNA1-6), or further away, at two upstream regulatory regions (gRNA7 and gRNA8) (Fig. 5A and B). First, we tested all possible combinations of four gRNAs (gRNA1-4) targeting the core promoter and found indeed that on its own one gRNA (gRNA3) is particularly efficient in activating *NEUROD1* transcription via dRNP-mediated gene induction in HAF cells, inducing transcript levels almost for three $\log_{10}$ scales after 24h (Fig. 5C). In contrast, RNP complexes built with either of the other three individually tested gRNAs (gRNA1, gRNA2 and gRNA4) had only a minor effect on *NEUROD1* expression (<20-fold induction). Nevertheless, adding either of those gRNAs to gRNA3 by dRNP-mediated target multiplexing, transcriptional output increased, way beyond merely additive effects (Fig. 5C). Next, we applied complexes build with each of the eight gRNAs and found that particularly those targeting more upstream sites were ineffective for activating *NEUROD1* transcription on their own. Nevertheless, combining several gRNAs with each other, resulted in disproportionately high gene induction rates, all in all scaling with the number of gRNAs combined (Fig. 5D). Combining all eight gRNAs together resulted in gene induction rates of more than 4 $\log_{10}$ scales (Fig. 5D).

RNP-mediated gene induction enables directing cell fate with high efficiency

To test, whether RNP-mediated gene induction is sufficient to affect cell fate, we applied dRNPs to human induced pluripotent stem cells (hiPSC) (Fig. 6A, Supplementary Methods S3). A single transfection of hiPSCs with dRNPs targeting either

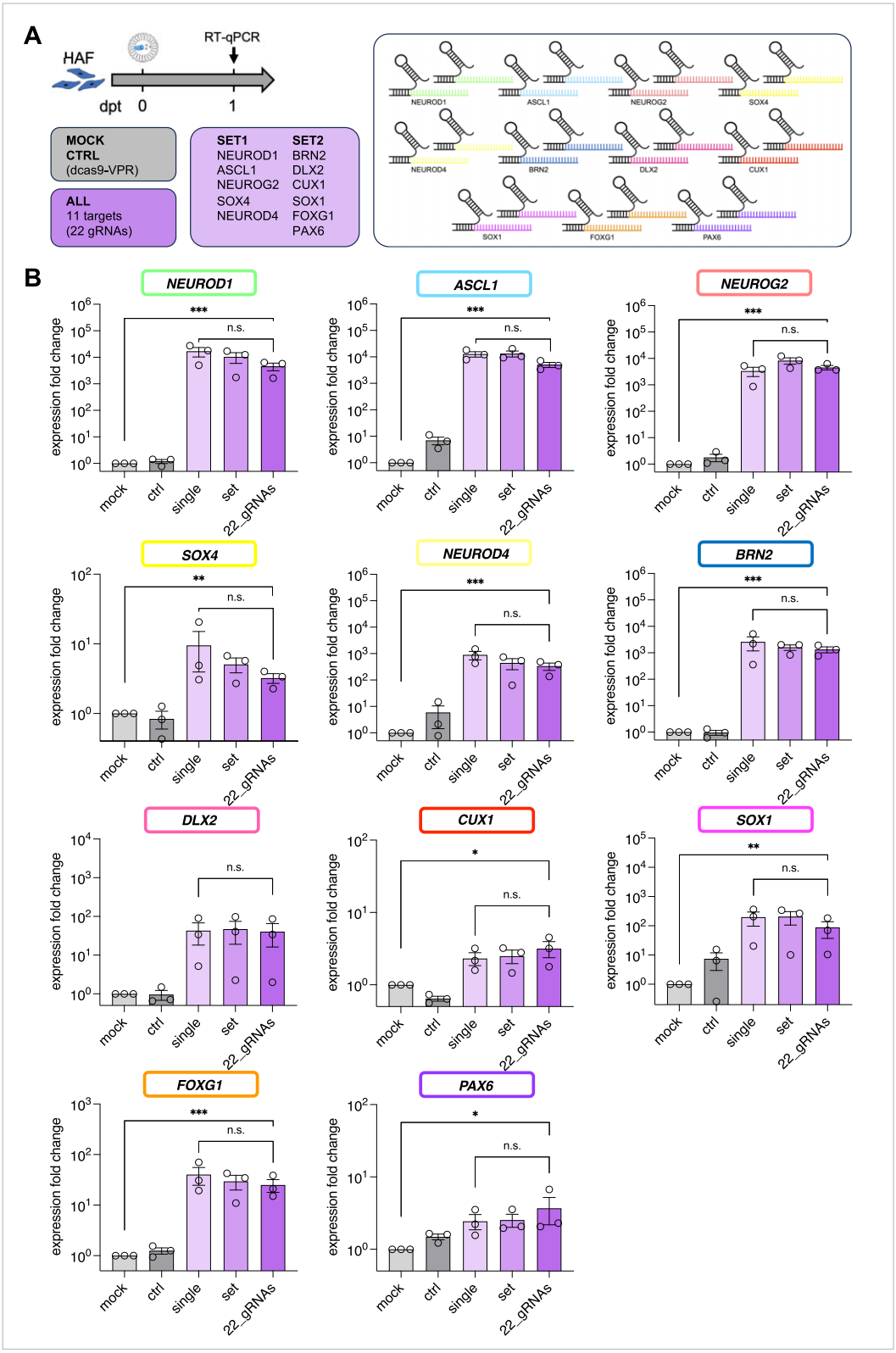

Figure 4. dRNPs can be used as a versatile tool for multiplexed gene activation. (**A**) Experimental design using a set of 22 gRNAs to simultaneously activate 11 target genes. (**B**) RT-qPCR analysis comparing the activation of a single gene (single) with combinations of sets of five or six genes (set) with multiplexed activation of 11 genes (22_gRNAs). Mock transfections (mock) and dCas9-VPR protein-only transfections (ctrl) were used as controls. Data are presented as mean ± S.E.M. ($n = 3$ independent experiments). Two-tailed t-test was performed for statistical analysis. * $P < 0.05$, ** $P < 0.01$.

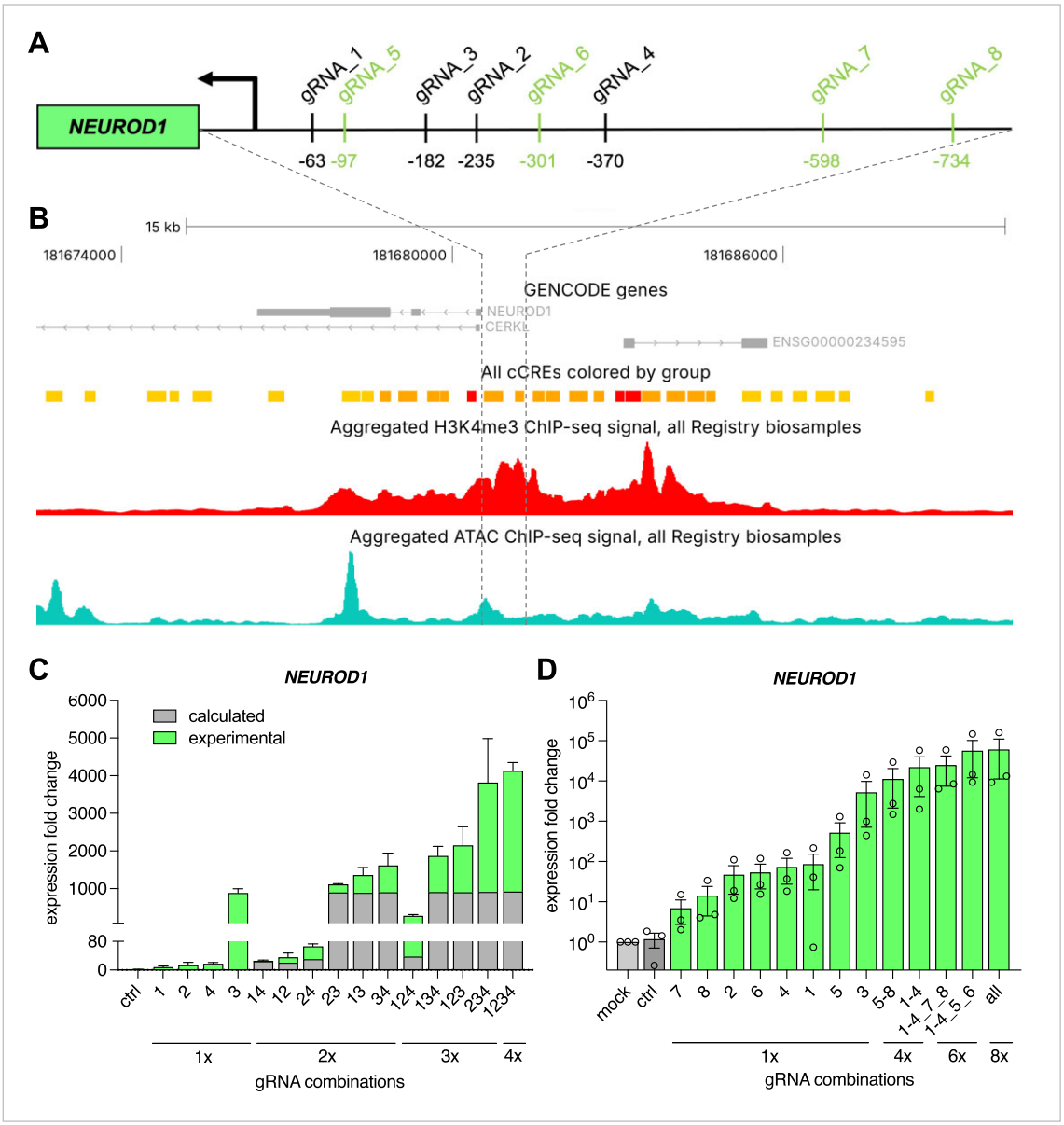

Figure 5. Multiplexed target gene activation via dRNPs reveals gRNA synergy. (**A**) Experimental design using 8 gRNAs to target the promoter region of *NEUROD1*. (**B**) Chromatin regulatory context derived from the ENCODE browser to display the regulatory features of the promoter region of *NEUROD1*. Tracks include histone modifications of active regulatory elements (H3K4me3) and ATAC profiles indicating open and accessible chromatin sites. (**C**) RT-qPCR analysis investigating the single and combined effects of four gRNAs 1 day after dRNP delivery. Calculated total expression as sum of sgRNA expression levels is indicated by grey/lower fraction of bars. Data are shown as mean and SD from technical triplicates. (**D**) Synergistic effect on *NEUROD1* expression using eight gRNAs. Mock transfections (mock) and dCas9-VPR protein-only transfections (ctrl) were used as controls. Data are presented as mean ± S.E.M. ($n = 3$ independent experiments).

NEUROD1 or *NEUROG2* resulted in a strong and immediate transcriptional activation of these genes as measured by RT-qPCR (Fig. 6D). Indeed, *NEUROD1* and *NEUROG2* mRNA level were elevated by 4–5 $\log_{10}$ scales on d1. During the following 5 days, expression levels declined roughly by 2 $\log_{10}$ scales. Furthermore, cross-activation between these two genes was observed, underlining their synergistic roles during neurogenesis. Interestingly, despite applying only a single dRNP delivery at d0, 6 days later, many newborn neurons were detected, positive for the pan-neuronal marker tubulin beta 3 class III (Tubb3) and the more mature marker microtubule associated protein 2 (Map2) (Fig. 6B and C). Moreover, the morphology and number of neuronal cells is comparable to those gained through transduction of retroviral vectors containing an engineered hyperactive version of *NEUROG2*, mutated on multiple phosphorylation sites [30, 51], which is continuously expressed during this period (Fig. 6B and C). This indicates that although the dRNP activities are short lived, they are strong enough that even single deliveries can initiate remarkable cellular changes.

Finally, we tested whether dRNPs are also potent enough to transdifferentiate fully differentiated cells. We made use of proliferating astrocyte populations (pAstrocytes) derived through a ~4 week protocol from human iPSCs [30]. Differentiation of pAstros from hiPSC resulted in a homogenous population of cells with glial morphology, consistently

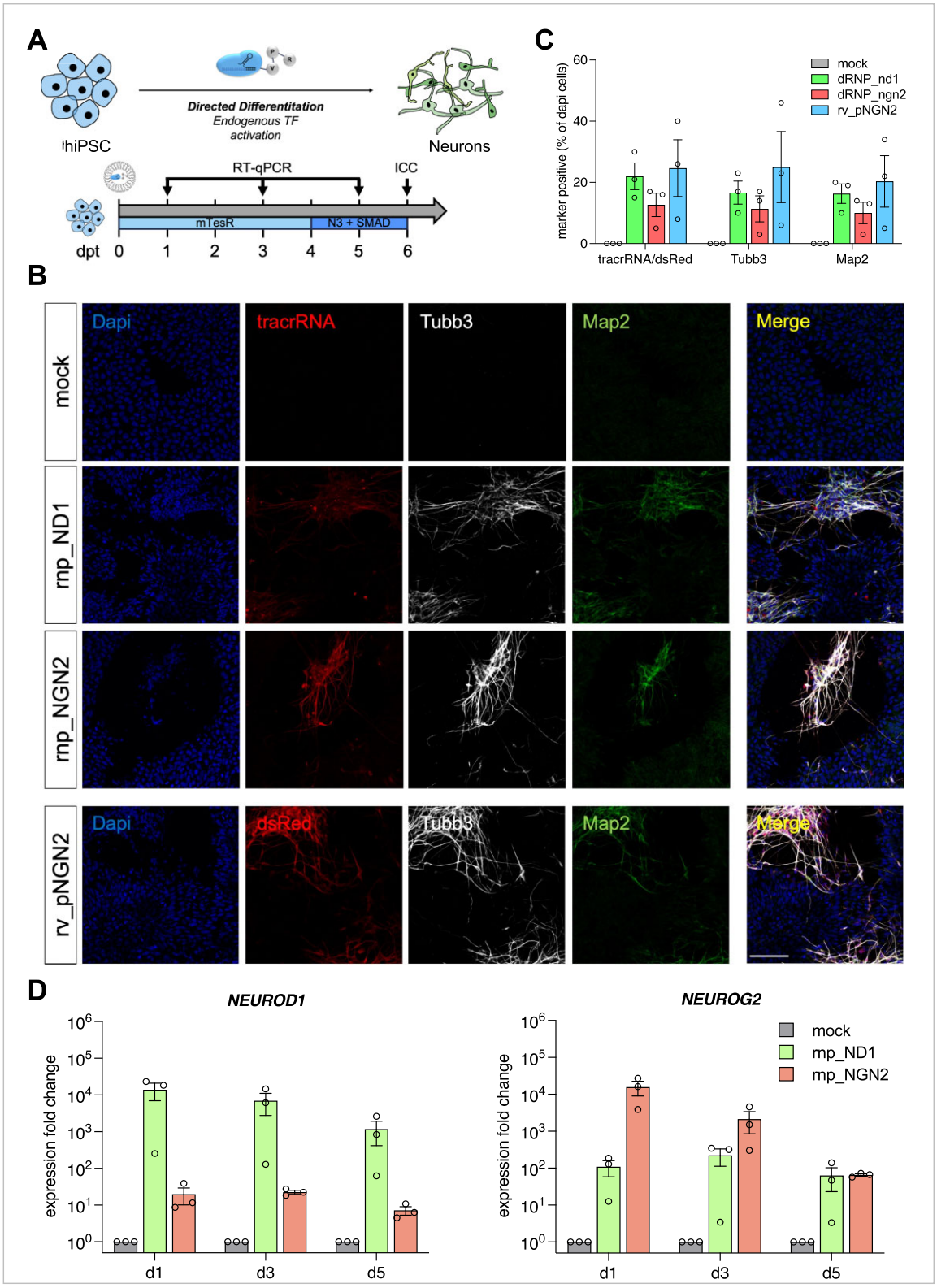

Figure 6. Transient RNP-based CRISPRa enables fast forward differentiation of human iPSCs into neurons. (**A**) Experimental design. Single deliveries of dRNPs are used to endogenously activate the neuronal transcription factors *NEUROD1* or *NEUROG2* in hiPSCs for neuronal fate induction. Retroviral overexpression of a phospho-incompetent version of Neurogenin-2 (rv_pNGN2) was used as positive control. (**B**) Representative immunofluorescence microscopy images of hiPSCs 6 days after dRNP transfection and retroviral transduction stained for the pan-neuronal marker tubulin beta 3 class III (Tubb3) and the mature neuronal marker microtubule associated protein 2 (Map2). ($n = 3$ independent experiments). Scale bar: 100 μm. (**C**) Quantification of (**B**). Percentage of marker positive cells relative to dapi on d6 of the experiment. Data are presented as mean ± S.E.M. ($n = 3$ independent experiments). (**D**) RT-qPCR analysis of dRNP-based transcriptional upregulation of *NEUROD1* and *NEUROG2* in hiPSCs following a single dRNP delivery. Data are presented as mean ± S.E.M. ($n = 3$ independent experiments).

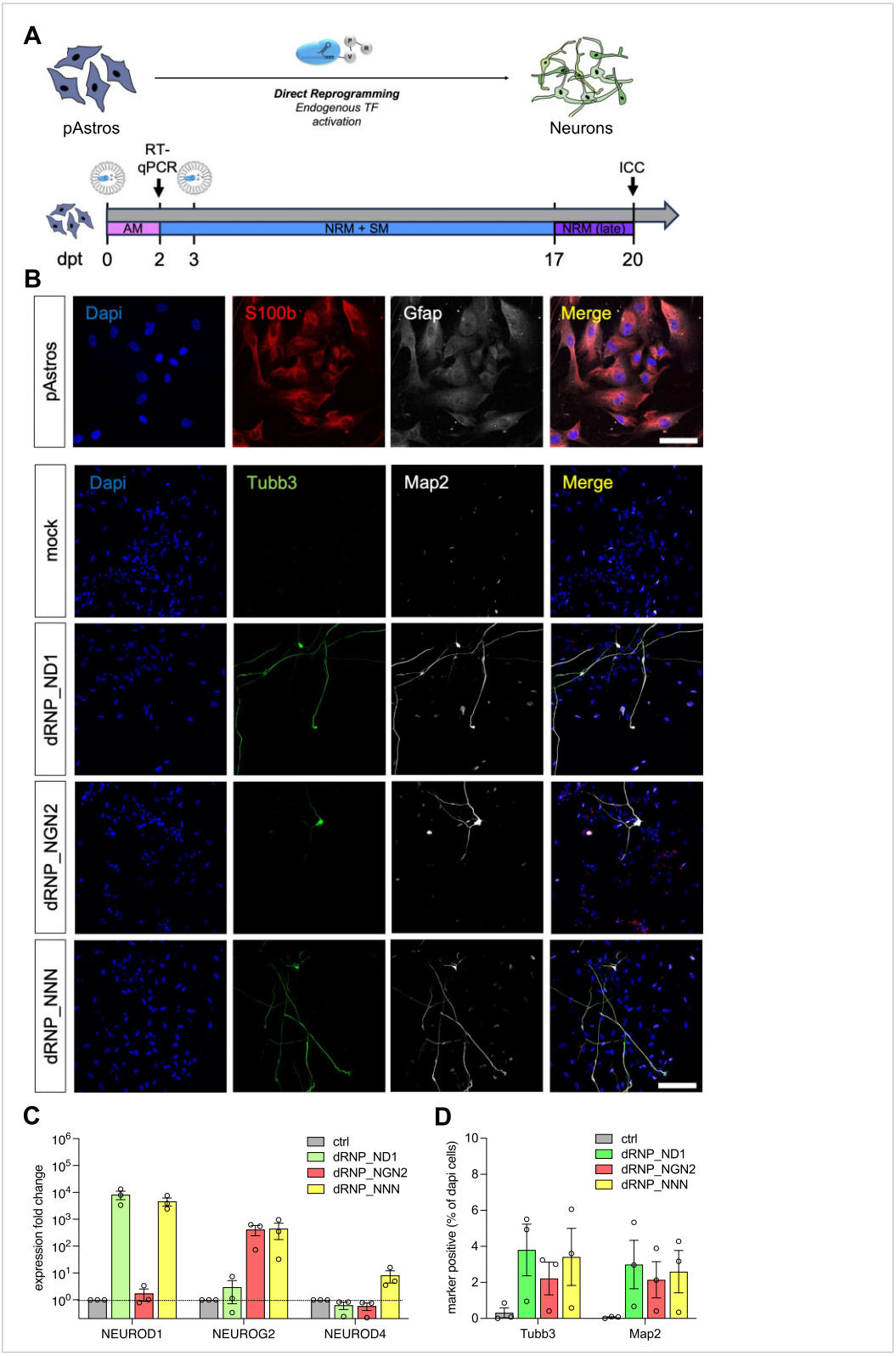

Figure 7. dRNP multiplexing of single and multiple TFs directly converts human iPSC-derived proliferating astrocytes (pAstros) into neurons. (**A**) Experimental design. Human pAstros are transfected with dRNPs on experimental days 0 and 3 of the experiment targeting *NEUROD1* (ND1), *NEUROG2* (NGN2) or a combination of *NEUROD1, NEUROG2 and NEUROD4* (NNN) at their promoter sites. (**B**) Representative Immunofluorescence microscopy images of differentiated pAstros stained for glial markers such as S100 calcium binding protein B (S100b) and glial fibrillary acidic protein (GFAP) and induced neurons 20 days after the first dRNP transfection. To detect new-born neurons, cells were stained for the pan-neuronal marker tubulin beta 3 class III (Tubb3) and the mature neuronal marker microtubule associated protein 2 (Map2) ($n = 3$ independent experiments). Scale bar: 100 μm. (**C**) RT-qPCR analysis of dRNP-based transcriptional upregulation of *NEUROD1*, *NEUROG2* and *NEUROD4* on day 2 of the experiment. Data are presented as mean ± S.E.M. ($n = 3$ independent experiments). (**D**) Quantification of (**B**).

expressing glial markers such as S100 calcium binding protein B (S100b) and glial fibrillary acidic protein (GFAP) (Fig. 7B). We transfected dRNPs twice, at d0 and d3, with the aim to activate either the reprogramming factor *NEUROG2* (NGN2), *NEUROD1* (ND1) or a combination of *NEUROG2*, *NEUROD1* and *NEUROD4* (NNN, Fig. 7A). qPCR analysis confirmed gene induction of the target genes at day 2 (Fig. 7C). On day 20 of the experiment, multiple cells with complex morphologies indicative of neurons were found among the dRNP treated cells while completely absent in control conditions (Fig. 7B). These cells were also strongly positive for Tubb3 and Map2, markers absent in control conditions (Fig. 7D), indicating that dRNPs are potent enough to achieve cell fate conversion even in terminally differentiated human cell populations.

Discussion

Here we introduce the generation, optimization and use of second generation CRISPRa RNPs (dRNPs). While the application of WT RNPs are very prevalent [52–55], the direct use of dCas9 for gene activation has been only reported in few cases [29]. The reported CRISPRa RNPs are based on first generation CRISPRa systems (e.g. dCas9-VP64), while dCas9-VPR protein could not been purified from bacterial cultures [18]. By switching to an insect-cell based expression system, we overcame this issue and demonstrate the efficient purification of a second generation CRISPRa protein, dCas9-VPR, which has been shown to be more potent [12]. We show that dCas9-VPR protein can be combined with any tested crRNA types to from functional ribonucleoprotein-complexes (dRNPs) for targeted gene activation. Applying our dRNPs to human cell lines, primary cells, stem cells and stem cell-derived cell models reveal remarkably efficient delivery and strong target gene induction. The cellular systems used in this study (astrocytes, fibroblasts and iPSCs) are all considered fast dividing for human diploid cells (estimated cell cycle lengths 40–48 h, 30–36 h, and 24–30 h, respectively). It will be interesting to explore how the dRNP half-life and efficacy are affected when applied to cells with lower proliferation rates (such as neurons) or species with faster cell cycle dynamics (such as murine cell types).

In addition, dRNPs surpass several limitations that alternative CRISPRa systems face, some technical, such as virus packaging capacity and gRNA cloning, others biological, such as speed and temporal resolution of gene induction. Notably, we find significant induction of gene expression already hours after dRNP delivery. We are confident, the transient nature of the dRNP system could serve as a powerful tool to investigate and manipulate gene regulatory networks with precise time resolution. dRNP-based transcriptional bursts at defined promoter sites would allow to investigate potential long-term effects on gene-regulatory elements such as epigenetic memory. Conventional transient gene regulatory approaches rely on inducing gene activation, e.g. via light or small molecules [45–47, 56–58]. Therefore, even though the time-resolution of these systems might be very sharp, combining several targets simultaneously or activating multiple genes sequentially is challenging; and more importantly, the target elements characterized are usually limited to genetically modified loci. In contrast, applying dRNPs allows the efficient activation of endogenous promoters with sharp time resolution and without the need for a priori genetic manipulation. Moreover, since synthetized gRNAs are inexpensive and commercially available, once protein has been purified, dRNPs are ready to be used for any target, in any species and cell type.

In this work, we also demonstrate that the dRNP-based approach offers the possibility to increase the number of gRNAs used to target one or multiple genes via extensive target multiplexing. CRISPRa has been shown to be well suited for multiplexed target activation, which has also been successfully achieved applying a number of strategies [9, 10, 18, 21, 48, 59]. With dRNPs the unimpeded use of at least 22 gRNAs appears to be possible, 35 gRNAs with some attenuation, and thus represents a novel tool promising to allow comprehensive manipulations of cellular transcriptional networks. Separate dRNP pre-assembly enables to robustly deliver equimolar ratios for each target region avoiding potential differences in assembly and/ or gRNA transcription efficiencies in the cells [9, 10]. Moreover, since gRNAs are inexpensively synthesized commercially, the dRNP-based approach overcomes limitations inflicted by cloning multiple gRNA cassettes into single vectors [5, 22]. Through optimization of dRNP generation, composition and delivery, we were able to show that dRNPs allow very strong targeted activation of transcription. This induction is specific and can be further increased by using chemically stabilized gRNAs. In line with recent insights based on plasmid based approaches [60], we find that gene activation was synergistically enhanced through targeting different regulatory elements of the same gene. More experiments are needed to reveal which molecular processes are involved in this, but it is tempting to speculate that phase-separated condensates may play a role [61]. Concerning the particularly preferable features of dRNPs, such as strong target gene induction, sharp time resolution, and extensive multiplexing potential, we did not yet reach limitations during the characterization and optimization of the technology. While we can show that the combination of 35 gRNAs is possible for the activation of multiple targets and 8 gRNAs synergize to induce a single target gene, this may not reflect the maximum that is technically achievable. We show that single inductions are potent enough to induce strong cellular effects days later, and multiple dRNP deliveries are possible. Indeed, we present evidence that dRNP activity is strong enough to enable the targeted manipulation of cell fate choice and cell identity, which is believed to be dependent on high expression levels of master transcription factors. Specifically, we demonstrate that dRNP admission and activation of neuronal reprogramming factors in human cells instructs the generation of new neurons.

Despite the presented advantages of dRNPs, there are disadvantages with this technology, too. The most evident issue is that, compared to AAV, options for *in vivo* delivery of dRNPs are limited. Nevertheless, even without such an option, the dRNP approach could be suitable for therapeutic strategies, applying *ex vivo* manipulation of patient cells [62], with the added benefit of ultimately transferring cells without DNA mutation, integration and/or virus expression. Moreover, since it has been shown for WT Cas9 that pre-assembled CRISPR-RNPs can be delivered very efficiently *in vitro* [52–54, 63, 64], and several novel *in vivo* delivery systems for RNPs have been recently reported [25, 65–67], dRNPs might offer a promising strategy for mutation-free, DNA-free and virus-free gene-therapeutic approaches.

Acknowledgements

We thank Nadine Fernandez-Novel Marx and Martina Bürkle for human iPSC culture and support on human pAstros differentiation and Matteo Puglisi for advice and support on setting up the dRNP approach. We acknowledge the Core Facility Flow Cytometry (CF FlowCyt) at the Biomedical Center, Ludwig-Maximilians-Universität München, and the Genomics Core Facility and the Protein Expression & Purification Facility of the Helmholtz Zentrum München (HMGU) for providing equipment, services, and expertise. We are particularly grateful to Prof. Rasmus O. Bak (Aarhus University) for sharing purified dCas9-VP64 protein samples.

Author contributions: T.S. (Conceptualization [equal], Data curation [equal], Formal analysis [equal], Investigation [lead], Methodology [equal], Writing - original draft [supporting], Writing - review & editing [supporting]), M.W. (Investigation [supporting], Methodology [supporting]), L.E. (Investigation [supporting], Methodology [supporting]), T.T.T. (Investigation [supporting], Methodology [supporting]), A.D. (Data curation [lead], Formal analysis [lead]), L.V. (Investigation [supporting], Validation [supporting]), S.I. (Investigation [supporting]), M.I.B. (Investigation [supporting]), D. (Investigation [supporting]), A.N. (Investigation [supporting]), A.K. (Conceptualization [supporting]), A.G. (Methodology [supporting]), A.S.D.M. (Methodology [equal], Supervision [supporting]), and S.H.S. (Conceptualization [lead], Funding acquisition [lead], Methodology [equal], Project administration [lead], Supervision [lead], Writing - original draft [lead], Writing - review & editing [lead]).

Supplementary data

Supplementary data is available at NAR online.

Conflict of interest

None declared.

Funding

T.S. is supported by EpiCrossBorders, International Helmholtz-Edinburgh Research School for Epigenetics. EpiCrossBorders is funded in equal parts by Helmholtz Zentrum München and the Helmholtz Association. S.H.S. acknowledges funding by DFG (STR 1385/5-1), the SFB "Chromatin Dynamics "INST 86/2110-1″, the EU / EIC (European Innovation Council) project REGENERAR (Ref:101129812), and the Frontiers in Research Fund (NRFR) Transformation grant funded through three Canadian federal funding agencies (Canadian Institutes of Health Research, the Natural Sciences and Engineering Research Council of Canada and Social Sciences, and the Humanities Research Council of Canada), iNeuron.

Data availability

The RNA-Seq data have been deposited in GEO under the accession number GSE288075. Raw data and material are available upon request.

References

1. Barrangou R, Fremaux C, Deveau H *et al.* CRISPR provides acquired resistance against viruses in prokaryotes. *Science* 2007;**315**:1709–12. https://doi.org/10.1126/science.1138140
2. Jinek M, Chylinski K, Fonfara I *et al.* A programmable dual-RNA-guided DNA endonuclease in adaptive bacterial immunity. *Science* 2012;**337**:816–21. https://doi.org/10.1126/science.1225829
3. Qi LS, Larson MH, Gilbert LA *et al.* Repurposing CRISPR as an RNA-guided platform for sequence-specific control of gene expression. *Cell* 2013;**152**:1173–83. https://doi.org/10.1016/j.cell.2013.02.022
4. La Russa MF, Qi LS. The new state of the art: cas9 for gene activation and repression. *Mol Cell Biol* 2015;**35**:3800–9. https://doi.org/10.1128/MCB.00512-15
5. Breunig CT, Koferle A, Neuner AM *et al.* CRISPR tools for physiology and cell State changes: potential of transcriptional engineering and epigenome editing. *Physiol Rev* 2021;**101**:177–211. https://doi.org/10.1152/physrev.00034.2019
6. Gilbert LA, Larson MH, Morsut L *et al.* CRISPR-mediated modular RNA-guided regulation of transcription in eukaryotes. *Cell* 2013;**154**:442–51. https://doi.org/10.1016/j.cell.2013.06.044
7. Maeder ML, Linder SJ, Cascio VM *et al.* CRISPR RNA-guided activation of endogenous human genes. *Nat Methods* 2013;**10**:977–9. https://doi.org/10.1038/nmeth.2598
8. Perez-Pinera P, Kocak DD, Vockley CM *et al.* RNA-guided gene activation by CRISPR-Cas9-based transcription factors. *Nat Methods* 2013;**10**:973–6. https://doi.org/10.1038/nmeth.2600
9. Cheng AW, Wang H, Yang H *et al.* Multiplexed activation of endogenous genes by CRISPR-on, an RNA-guided transcriptional activator system. *Cell Res* 2013;**23**:1163–71. https://doi.org/10.1038/cr.2013.122
10. Konermann S, Brigham MD, Trevino AE *et al.* Genome-scale transcriptional activation by an engineered CRISPR-Cas9 complex. *Nature* 2015;**517**:583–8. https://doi.org/10.1038/nature14136
11. Tanenbaum ME, Gilbert LA, Qi LS *et al.* A protein-tagging system for signal amplification in gene expression and fluorescence imaging. *Cell* 2014;**159**:635–46. https://doi.org/10.1016/j.cell.2014.09.039
12. Chavez A, Scheiman J, Vora S *et al.* Highly efficient Cas9-mediated transcriptional programming. *Nat Methods* 2015;**12**:326–8. https://doi.org/10.1038/nmeth.3312
13. Pandelakis M, Delgado E, Ebrahimkhani MR. CRISPR-based synthetic transcription factors In Vivo: the future of therapeutic cellular programming. *Cell Syst* 2020;**10**:1–14. https://doi.org/10.1016/j.cels.2019.10.003
14. Villiger L, Joung J, Koblan L *et al.* CRISPR technologies for genome, epigenome and transcriptome editing. *Nat Rev Mol Cell Biol* 2024;**25**:464–87. https://doi.org/10.1038/s41580-023-00697-6
15. Zheng R, Zhang L, Parvin R *et al.* Progress and perspective of CRISPR-Cas9 technology in translational medicine. *Adv Sci* 2023;**10**:e2300195. https://doi.org/10.1002/advs.202300195
16. Zhou M, Tao X, Sui M *et al.* Reprogramming astrocytes to motor neurons by activation of endogenous Ngn2 and Isl1. *Stem Cell Rep* 2021;**16**:1777–91. https://doi.org/10.1016/j.stemcr.2021.05.020
17. Liu S, Striebel J, Pasquini G *et al.* Neuronal cell-type engineering by transcriptional activation. *Front Genome Ed* 2021;**3**:715697. https://doi.org/10.3389/fgeed.2021.715697
18. Black JB, Adler AF, Wang HG *et al.* Targeted epigenetic remodeling of endogenous loci by CRISPR/Cas9-based transcriptional activators directly converts fibroblasts to neuronal cells. *Cell Stem Cell* 2016;**19**:406–14. https://doi.org/10.1016/j.stem.2016.07.001
19. Shakirova KM, Ovchinnikova VY, Dashinimaev EB. Cell reprogramming with CRISPR/Cas9 based transcriptional regulation systems. *Front Bioeng Biotechnol* 2020;**8**:882. https://doi.org/10.3389/fbioe.2020.00882
20. Black JB, McCutcheon SR, Dube S *et al.* Master regulators and cofactors of human neuronal cell fate specification identified by

CRISPR gene activation screens. *Cell Rep* 2020;**33**:108460. https://doi.org/10.1016/j.celrep.2020.108460
21. Zhou H, Liu J, Zhou C *et al.* In vivo simultaneous transcriptional activation of multiple genes in the brain using CRISPR-dCas9-activator transgenic mice. *Nat Neurosci* 2018;**21**:440–6. https://doi.org/10.1038/s41593-017-0060-6
22. Campa CC, Weisbach NR, Santinha AJ *et al.* Multiplexed genome engineering by Cas12a and CRISPR arrays encoded on single transcripts. *Nat Methods* 2019;**16**:887–93. https://doi.org/10.1038/s41592-019-0508-6
23. Truong DJ, Kuhner K, Kuhn R *et al.* Development of an intein-mediated split-Cas9 system for gene therapy. *Nucleic Acids Res* 2015;**43**:6450–8. https://doi.org/10.1093/nar/gkv601
24. Chew WL, Tabebordbar M, Cheng JK *et al.* A multifunctional AAV-CRISPR-Cas9 and its host response. *Nat Methods* 2016;**13**:868–74. https://doi.org/10.1038/nmeth.3993
25. Chen K, Stahl EC, Kang MH *et al.* Engineering self-deliverable ribonucleoproteins for genome editing in the brain. *Nat Commun* 2024;**15**:1727. https://doi.org/10.1038/s41467-024-45998-2
26. Hussain W, Mahmood T, Hussain J *et al.* CRISPR/Cas system: a game changing genome editing technology, to treat human genetic diseases. *Gene* 2019;**685**:70–5. https://doi.org/10.1016/j.gene.2018.10.072
27. Doudna JA. The promise and challenge of therapeutic genome editing. *Nature* 2020;**578**:229–36. https://doi.org/10.1038/s41586-020-1978-5
28. Pandey H, Yadav B, Shah K *et al.* A new method for the robust expression and single-step purification of dCas9 for CRISPR interference/activation (CRISPRi/a) applications. *Protein Expr Purif* 2024;**220**:106500. https://doi.org/10.1016/j.pep.2024.106500
29. Jensen TI, Mikkelsen NS, Gao Z *et al.* Targeted regulation of transcription in primary cells using CRISPRa and CRISPRi. *Genome Res* 2021;**31**:2120–30. https://doi.org/10.1101/gr.275607.121
30. Sonsalla G, Malpartida AB, Riedemann T *et al.* Direct neuronal reprogramming of NDUFS4 patient cells identifies the unfolded protein response as a novel general reprogramming hurdle. *Neuron* 2024;**112**:1117–32. https://doi.org/10.1016/j.neuron.2023.12.020
31. Labun K, Montague TG, Krause M *et al.* CHOPCHOP v3: expanding the CRISPR web toolbox beyond genome editing. *Nucleic Acids Res* 2019;**47**:W171–4. https://doi.org/10.1093/nar/gkz365
32. Livak KJ, Schmittgen TD. Analysis of relative gene expression data using real-time quantitative PCR and the 2(-Delta Delta C(T)) method. *Methods* 2001;**25**:402–8. https://doi.org/10.1006/meth.2001.1262
33. Schindelin J, Arganda-Carreras I, Frise E *et al.* Fiji: an open-source platform for biological-image analysis. *Nat Methods* 2012;**9**:676–82. https://doi.org/10.1038/nmeth.2019
34. Bolger AM, Lohse M, Usadel B. Trimmomatic: a flexible trimmer for Illumina sequence data. *Bioinformatics* 2014;**30**:2114–20. https://doi.org/10.1093/bioinformatics/btu170
35. Dobin A, Davis CA, Schlesinger F *et al.* STAR: ultrafast universal RNA-seq aligner. *Bioinformatics* 2013;**29**:15–21. https://doi.org/10.1093/bioinformatics/bts635
36. Danecek P, Bonfield JK, Liddle J *et al.* Twelve years of SAMtools and BCFtools. *Gigascience* 2021;**10**:giab008. https://doi.org/10.1093/gigascience/giab008
37. Anders S, Pyl PT, Huber W. HTSeq–a Python framework to work with high-throughput sequencing data. *Bioinformatics* 2015;**31**:166–9. https://doi.org/10.1093/bioinformatics/btu638
38. Badia IMP, Velez Santiago J, Braunger J *et al.* decoupleR: ensemble of computational methods to infer biological activities from omics data. *Bioinform Adv* 2022;**2**:vbac016. https://doi.org/10.1093/bioadv/vbac016
39. Wolf FA, Angerer P, Theis FJ. SCANPY: large-scale single-cell gene expression data analysis. *Genome Biol* 2018;**19**:15. https://doi.org/10.1186/s13059-017-1382-0
40. Muzellec B, Telenczuk M, Cabeli V *et al.* PyDESeq2: a python package for bulk RNA-seq differential expression analysis. *Bioinformatics* 2023;**39**:btad547. https://doi.org/10.1093/bioinformatics/btad547
41. Bocchi R, Masserdotti G, Gotz M. Direct neuronal reprogramming: fast forward from new concepts toward therapeutic approaches. *Neuron* 2022;**110**:366–93. https://doi.org/10.1016/j.neuron.2021.11.023
42. Baumann V, Wiesbeck M, Breunig CT *et al.* Targeted removal of epigenetic barriers during transcriptional reprogramming. *Nat Commun* 2019;**10**:2119. https://doi.org/10.1038/s41467-019-10146-8
43. Maetzel D, Denzel S, Mack B *et al.* Nuclear signalling by tumour-associated antigen EpCAM. *Nat Cell Biol* 2009;**11**:162–71. https://doi.org/10.1038/ncb1824
44. Concordet JP, Haeussler M. CRISPOR: intuitive guide selection for CRISPR/Cas9 genome editing experiments and screens. *Nucleic Acids Res* 2018;**46**:W242–5. https://doi.org/10.1093/nar/gky354
45. Legnini I, Emmenegger L, Zappulo A *et al.* Spatiotemporal, optogenetic control of gene expression in organoids. *Nat Methods* 2023;**20**:1544–52. https://doi.org/10.1038/s41592-023-01986-w
46. Polstein LR, Gersbach CA. A light-inducible CRISPR-Cas9 system for control of endogenous gene activation. *Nat Chem Biol* 2015;**11**:198–200. https://doi.org/10.1038/nchembio.1753
47. Nihongaki Y, Furuhata Y, Otabe T *et al.* CRISPR-Cas9-based photoactivatable transcription systems to induce neuronal differentiation. *Nat Methods* 2017;**14**:963–6. https://doi.org/10.1038/nmeth.4430
48. Breunig CT, Durovic T, Neuner AM *et al.* One step generation of customizable gRNA vectors for multiplex CRISPR approaches through string assembly gRNA cloning (STAgR). *PLoS One* 2018;**13**:e0196015. https://doi.org/10.1371/journal.pone.0196015
49. Mahata B, Cabrera A, Brenner DA *et al.* Compact engineered human mechanosensitive transactivation modules enable potent and versatile synthetic transcriptional control. *Nat Methods* 2023;**20**:1716–28. https://doi.org/10.1038/s41592-023-02036-1
50. Mali P, Aach J, Stranges PB *et al.* CAS9 transcriptional activators for target specificity screening and paired nickases for cooperative genome engineering. *Nat Biotechnol* 2013;**31**:833–8. https://doi.org/10.1038/nbt.2675
51. Ali F, Hindley C, McDowell G *et al.* Cell cycle-regulated multi-site phosphorylation of neurogenin 2 coordinates cell cycling with differentiation during neurogenesis. *Development* 2011;**138**:4267–77. https://doi.org/10.1242/dev.067900
52. Kim S, Kim D, Cho SW *et al.* Highly efficient RNA-guided genome editing in human cells via delivery of purified Cas9 ribonucleoproteins. *Genome Res* 2014;**24**:1012–9. https://doi.org/10.1101/gr.171322.113
53. Lin S, Staahl BT, Alla RK *et al.* Enhanced homology-directed human genome engineering by controlled timing of CRISPR/Cas9 delivery. *eLife* 2014;**3**:e04766. https://doi.org/10.7554/eLife.04766
54. Zuris JA, Thompson DB, Shu Y *et al.* Cationic lipid-mediated delivery of proteins enables efficient protein-based genome editing in vitro and in vivo. *Nat Biotechnol* 2015;**33**:73–80. https://doi.org/10.1038/nbt.3081
55. Frangoul H, Altshuler D, Cappellini MD *et al.* CRISPR-Cas9 gene editing for Sickle cell disease and beta-thalassemia. *N Engl J Med* 2021;**384**:252–60. https://doi.org/10.1056/NEJMoa2031054
56. Pickar-Oliver A, Gersbach CA. The next generation of CRISPR-Cas technologies and applications. *Nat Rev Mol Cell Biol* 2019;**20**:490–507. https://doi.org/10.1038/s41580-019-0131-5
57. Thakore PI, Black JB, Hilton IB *et al.* Editing the epigenome: technologies for programmable transcription and epigenetic modulation. *Nat Methods* 2016;**13**:127–37. https://doi.org/10.1038/nmeth.3733
58. Bubeck F, Hoffmann MD, Harteveld Z *et al.* Engineered anti-CRISPR proteins for optogenetic control of CRISPR-Cas9.

Nat Methods 2018;**15**:924–7. https://doi.org/10.1038/s41592-018-0178-9
59. Giehrl-Schwab J, Giesert F, Rauser B *et al.* Parkinson's disease motor symptoms rescue by CRISPRa-reprogramming astrocytes into GABAergic neurons. *EMBO Mol Med* 2022;**14**:e14797. https://doi.org/10.15252/emmm.202114797
60. Tak YE, Horng JE, Perry NT *et al.* Augmenting and directing long-range CRISPR-mediated activation in human cells. *Nat Methods* 2021;**18**:1075–81. https://doi.org/10.1038/s41592-021-01224-1
61. Boija A, Klein IA, Sabari BR *et al.* Transcription factors activate genes through the phase-separation capacity of their activation domains. *Cell* 2018;**175**:1842–55. https://doi.org/10.1016/j.cell.2018.10.042
62. Alsaiari SK, Eshaghi B, Du B *et al.* CRISPR–Cas9 delivery strategies for the modulation of immune and non-immune cells. *Nat Rev Mater* 2025;**10**:44–61. https://doi.org/10.1038/s41578-024-00725-7
63. Kouranova E, Forbes K, Zhao G *et al.* CRISPRs for optimal targeting: delivery of CRISPR components as DNA, RNA, and protein into cultured cells and single-cell embryos. *Hum Gene Ther* 2016;**27**:464–75. https://doi.org/10.1089/hum.2016.009
64. Mout R, Ray M, Yesilbag Tonga G *et al.* Direct cytosolic delivery of CRISPR/Cas9-Ribonucleoprotein for efficient gene editing. *ACS Nano* 2017;**11**:2452–8. https://doi.org/10.1021/acsnano.6b07600
65. Finn JD, Smith AR, Patel MC *et al.* A single administration of CRISPR/Cas9 lipid nanoparticles achieves robust and persistent *in vivo* genome editing. *Cell Rep* 2018;**22**:2227–35. https://doi.org/10.1016/j.celrep.2018.02.014
66. Staahl BT, Benekareddy M, Coulon-Bainier C *et al.* Efficient genome editing in the mouse brain by local delivery of engineered Cas9 ribonucleoprotein complexes. *Nat Biotechnol* 2017;**35**:431–4. https://doi.org/10.1038/nbt.3806
67. Simoes S, Lino M, Barrera A *et al.* Near-infrared light activated formulation for the spatially controlled release of CRISPR-Cas9 Ribonucleoprotein for brain gene editing. *Angew Chem Int Ed* 2024;**63**:e202401004. https://doi.org/10.1002/anie.202401004

Received: August 14, 2024. **Revised:** March 3, 2025. **Editorial Decision:** March 4, 2025. **Accepted:** March 17, 2025